Measurement of η meson decays into lepton-antilepton pairs

M. Berłowski,[1] Chr. Bargholtz,[2] M. Bashkanov,[3] D. Bogoslawsky,[4] A. Bondar,[5] H. Calén,[6] F. Cappellaro,[7] H. Clement,[3] L. Demirörs,[8] C. Ekström,[6] K. Fransson,[6] L. Gerén,[2] L. Gustafsson,[7] B. Höistad,[7] G. Ivanov,[4] M. Jacewicz,[7] E. Jiganov,[4] T. Johansson,[7] S. Keleta,[7] I. Koch,[7] S. Kullander,[7] A. Kupść,[6] A. Kuzmin,[5] A. Kuznetsov,[4] I.V. Laukhin,[9] K. Lindberg,[2] P. Marciniewski,[6] R. Meier,[3] B. Morosov,[4] W. Oelert,[10] C. Pauly,[8] H. Pettersson,[7] Y. Petukhov,[4] A. Povtorejko,[4] R.J.M.Y. Ruber,[6] K. Schönning,[7] W. Scobel,[8] R. Shafigullin,[9] B. Shwartz,[5] T. Skorodko,[3] V. Sopov,[11] J. Stepaniak,[1] P.-E. Tegnér,[2] P. Thörngren Engblom,[7] V. Tikhomirov,[4] A. Turowiecki,[12] G.J. Wagner,[3] M. Wolke,[10] A. Yamamoto,[13] J. Zabierowski,[1] I. Zartova,[2] and J. Złomańczuk[7]

(CELSIUS/WASA Collaboration)

[1] *The Andrzej Soltan Institute for Nuclear Studies, Warsaw and Lodz, Poland*
[2] *Stockholm University, Stockholm, Sweden*
[3] *Physikalisches Institut der Universität Tübingen, Tübingen, Germany*
[4] *Joint Institute for Nuclear Research, Dubna, Russia*
[5] *Budker Institute of Nuclear Physics, Novosibirsk, Russia*
[6] *The Svedberg Laboratory, Uppsala, Sweden*
[7] *Uppsala University, Uppsala, Sweden*
[8] *Institut für Experimentalphysik der Universität Hamburg, Hamburg, Germany*
[9] *Moscow Engineering Physics Institute, Moscow, Russia*
[10] *Institut für Kernphysik, Forschungszentrum Jülich, Jülich, Germany*
[11] *Institute of Theoretical and Experimental Physics, Moscow, Russia*
[12] *Institute of Experimental Physics, Warsaw, Poland*
[13] *High Energy Accelerator Research Organization, Tsukuba, Japan*

(Dated: February 17, 2013)

A search for rare lepton decays of the η meson was performed using the WASA detector at CELSIUS. Two candidates for double Dalitz decay $\eta \to e^+e^-e^+e^-$ events are reported with a background of 1.3±0.2 events. This allows to set an upper limit to the branching ratio of 9.7×10^{-5} (90% CL). The branching ratio for the decay $\eta \to e^+e^-\gamma$ is determined to $(7.8 \pm 0.5_{stat} \pm 0.8_{syst}) \times 10^{-3}$ in agreement with world average value. An upper limit (90% CL) for the branching ratio for the $\eta \to e^+e^-$ decay is 2.7×10^{-5} and a limit for the sum of the $\eta \to \mu^+\mu^-\mu^+\mu^-$ and $\eta \to \pi^+\pi^-\mu^+\mu^-$ decays is 3.6×10^{-4}.

PACS numbers: 13.20.-v, 14.40.Aq
Keywords: η meson decays, Dalitz decays

I. INTRODUCTION

The η decays with lepton pairs are closely related to the channels with real photons. A direct consequence of Quantum Electrodynamics is that a process with a real photon should be accompanied by a process where a virtual photon converts internally into a lepton-antilepton pair (fig. 1a,b). This fact was first pointed out by Dalitz in 1951 [1]. The decays can be related to the corresponding radiative decays with one or two photons using Quantum Electrodynamics and by introducing a function of the four momentum transfer squared of the virtual photons ($q^2_{1,2}$): $F(q_1^2, q_2^2, m_\eta^2)$ – the transion *Form Factor* (FF) (an overview is given e.g. in [2]). The $q^2_{1,2}$ for the Dalitz decay is equal to the invariant mass squared of the lepton-antilepton pair and $q^2_{1,2} \geq 4m_l^2$. The FF describes the structure of the transition region and it is also used for the process $\gamma^*\gamma^* \to \eta$ where $q^2_{1,2} < 0$ (space-like virtual photons).

Experimental information is scarce even for not so rare η meson decays with electron-positron pair(s) as seen in table I, where measured and predicted branching ratios (BR) are summarized. Even the branching ratio for the $\eta \to e^+e^-\gamma$ decay is known with a rather large uncertainty $(6.0 \pm 0.8) \times 10^{-3}$ [7]. It is worth noting that the quoted value was obtained as the average of two experimental results with a rather large scale factor – 1.4. The recent result from the CLEO Collaboration $(9.4 \pm 0.7) \times 10^{-3}$ [13] is larger by three standard deviations. None of the η decays with double lepton-antilepton pairs were observed so far. The decays were studied theoretically already 40 years ago by Jarlskog and Pilkhun [8] assuming a FF equal to one. The effect of the FF on the BR is expected to be less than 10% for the decay $\eta \to e^+e^-e^+e^-$ [11]. For decays with $\mu^+\mu^-$ pair(s) the influence is larger since only large q^2 values are probed.

Decays of neutral pseudoscalar mesons into a lepton-antilepton pair, $P \to \ell^+\ell^-$, represent a potentially important channel to look for effects of physics beyond the Standard Model [5]. The dominant mechanism within the Standard Model is a second order electromagnetic process, additionally suppressed by helicity conservation, involving two virtual photons $P \to \gamma^*\gamma^*$ shown in fig. 1c. Due to the loop appearing in the diagram the decay is sensitive to the values of the FF for any $q^2_{1,2}$ of the photons in the loop [14]. The imaginary part of the decay

Decay mode	BR exp.	BR theor.	Remarks
$\eta \to e^+e^-\gamma$	$(6.0 \pm 0.8) \times 10^{-3}$	$(6.37 - 6.57) \times 10^{-3}$	
$\eta \to \mu^+\mu^-\gamma$	$(3.1 \pm 0.4) \times 10^{-4}$	$(2.10 - 3.05) \times 10^{-4}$	
$\eta \to e^+e^-e^+e^-$	$< 6.9 \times 10^{-5}$	$(2.52 - 2.64) \times 10^{-5}$	Data CMD-2[3]
$\eta \to e^+e^-\mu^+\mu^-$	–	$(1.57 - 2.21) \times 10^{-7}$	
$\eta \to \mu^+\mu^-\mu^+\mu^-$	–	2.4×10^{-9}	
$\eta \to e^+e^-$	$< 7.7 \times 10^{-5}$	$\geq 1.7 \times 10^{-9}$	Data CLEO II[4], Unitarity bound [5]
$\eta \to \mu^+\mu^-$	$(5.8 \pm 0.8) \times 10^{-6}$	$\geq 4.3 \times 10^{-6}$	Unitarity bound [5]
$\eta \to \pi^+\pi^-e^+e^-$	$(4.3 \pm 1.3 \pm 0.4) \times 10^{-4}$	$(3.0 - 3.6) \times 10^{-4}$	Data CELSIUS/WASA [6]
$\eta \to \pi^+\pi^-\mu^+\mu^-$	–	7.5×10^{-9}	
$\eta \to \mu^\pm e^\mp$	$< 6 \times 10^{-6}$	0	Violates Lepton Flavor

TABLE I: The measured and calculated branching ratios for different η decay channels with lepton-antilepton pair(s). The data are from [7] if not stated otherwise. The upper limits are for 90% CL. Calculations for single and double Dalitz decays are from [8, 9, 10, 11, 12].

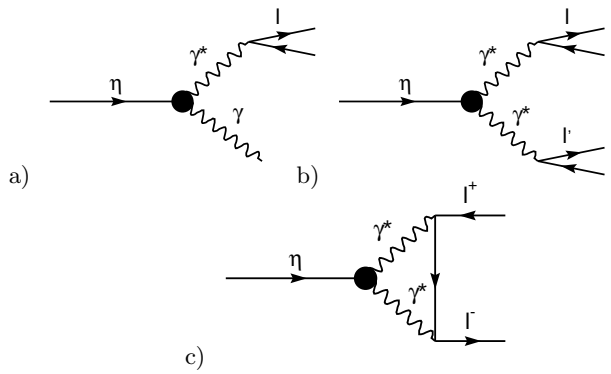

FIG. 1: Diagrams for a) single, b) double Dalitz decays of a neutral pseudoscalar meson (π^0, η or η') and c) dominating conventional mechanism for decay into a lepton-antilepton pair.

amplitude can be uniquely related to the decay width of the $\eta \to \gamma\gamma$ decay. The experimental value of $\Gamma(\eta \to \gamma\gamma)$ leads to a lower limit (the unitarity bound) of the branching ratio: BR$(\eta \to e^+e^-) \geq 1.7 \times 10^{-9}$ when the real part of the decay amplitude is neglected [2, 5]. This value is much lower than for other decays of π^0 and η into lepton-antilepton pairs. This makes the $\eta \to e^+e^-$ decay rate sensitive to a possible exotic contribution. The best experimental upper limit for the $BR(\eta \to e^+e^-)$ comes from the CLEO II collaboration [4] and is four orders of magnitude higher (table I). The decays $\pi^0 \to e^+e^-$, $\eta \to \mu^+\mu^-$ and $\eta \to e^+e^-$ are also important in order to estimate long range contribution to the decay $K_L \to \mu^+\mu^-$. The loop diagram of the short-distance amplitude is sensitive to the presence of a virtual top quark and could be used to improve the knowledge on the $|V_{td}|$ element of the CKM matrix [15, 16].

The real part of the amplitude of the $\eta \to e^+e^-$ decay can be estimated using the measured value of BR$(\eta \to \mu^+\mu^-)$ [15, 17, 18]. The assumption that the ratio between Im and Re parts of the amplitudes for the decays is the same leads to the prediction $BR(\eta \to e^+e^-) \approx (6 \pm 0.2) \times 10^{-9}$. A new, unknown process could increase the value. Recently the interest in the decays was revived due to the observed excess rate of the $\pi^0 \to e^+e^-$ decay [19] with respect to the Standard Model predictions [20] what triggered theoretical speculations that the excess might be caused by a neutral vector meson responsible for annihilation of a neutral scalar dark matter particle [21]. The consequence could be large (even an oder of magnitude) enhancement of the $\eta \to e^+e^-$ decay rate.

The plan of this paper is the following: In part II, the experiment is described and the data selection is presented. In section II.A the $\eta \to \pi^0\pi^0\pi^0$ decay where one of the neutral pions decays via $\pi^0 \to e^+e^-\gamma$ ($\eta \to \pi^0\pi^0\pi^0_D$) is presented. The process is used to verify the understanding of the detector response for electrons and positrons and to provide normalization for the BR of leptonic η decays. This is an extension of the systematical studies from a previous publication that used the same data sample [6]. In section III.A the Dalitz decay $\eta \to e^+e^-\gamma$ is considered and the BR is determined. In sections III.B to III.D the results of the search for the $\eta \to e^+e^-e^+e^-$, $\eta \to \mu^+\mu^-\mu^+\mu^-$, $\eta \to \pi^+\pi^-\mu^+\mu^-$ and $\eta \to e^+e^-$ decays are presented.

II. THE EXPERIMENT

The experiment was performed at the CELSIUS storage ring in Uppsala, using the WASA detector setup (fig. 2) [22]. Protons with a kinetic energy of 893 MeV interacted with frozen droplets of deuterium [23]. The η mesons were produced in the reaction $pd \to {}^3\mathrm{He}\,\eta$ close to the η production threshold. The detection of ^{3}He ions in a zero-degree spectrometer (tagging detector) provided a clean η trigger independent of decay channel [24]. The ^{3}He ions were identified and their energy was measured which allowed a clean selection of the $pd \to {}^3\mathrm{He}\,\eta$ reaction with a background (mainly due to $pd \to {}^3\mathrm{He}\pi\pi$ reaction) of about 1%. The tagging detector provided a few triggers per second (at a luminosity of $5 \times 10^{30} cm^{-2} s^{-1}$),

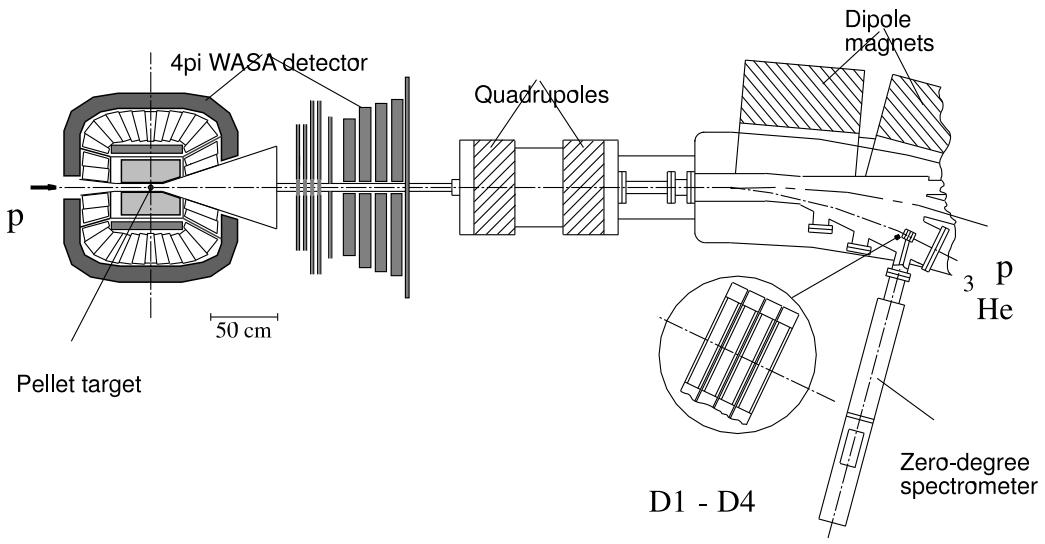

FIG. 2: The WASA detector with zero-degree spectrometer using CELSIUS dipoles.

yielding on average one recorded η event per second. During the two weeks of experiment (distributed over a period of half a year) nearly 3×10^5 η events were collected.

The charged η decay products were tracked using a cylindrical mini drift chamber (MDC), consisting of 17 layers of thin-walled (25μm) aluminized mylar tubes and built around a beryllium beam pipe of 60 mm diameter with wall thickness of only 1.2 mm (3.4×10^{-3} radiation lengths). Since the target deuterium droplets have a radius of 17μm (2×10^{-6} radiation lengths) the beam pipe is the most important source of photon conversion background. For example the fraction of e^+e^- pairs from $\eta \to \gamma\gamma$ with external photon conversion in the beam pipe to the Dalitz pairs from $\eta \to e^+e^-\gamma$ is about 60%. This background could be further suppressed by checking the reconstructed position of the vertex of a pair. The above features of the WASA detector are crucial for the investigation of reactions with e^+e^- pairs. The MDC is placed inside of a superconducting solenoid which provides a magnetic field of 1T. The MDC is surrounded by a barrel of plastic scintillators used mainly to define event start time for drift time reconstruction in the MDC. An electromagnetic calorimeter consisting of 1012 CsI(Na) crystals measures the energies of photons and their impact points.

Tracks of electrons and charged pions are reconstructed in MDC with an efficiency of about 80% if the transverse particle momenta are larger than about 20 MeV/c. One should stress that even lepton-antilepton pairs with parallel momenta (and thus minimal value of the invariant mass) could be efficiently measured in the MDC. The track reconstruction algorithm for the MDC used in the present studies was based on a global method of pattern recognition in which a constant magnetic field was assumed. The position resolution of the reconstructed vertex is about 0.05 cm FWHM in the plane perpendicular to the beam and 0.7 cm FWHM along the beam.

In the offline analysis, events with at least two charged particle tracks reconstructed in the MDC were required. Events with the tracks originating far from the beam target interaction region were rejected. Hit clusters in the calorimeter, without associated tracks in the MDC and with energy deposit larger than 20 MeV were assumed to originate from photons. Only events containing decay particle candidates with balanced electric charge were accepted for further analysis. The results on the $\eta \to \pi^+\pi^-e^+e^-$ decay channel were already presented earlier [6]. Events with a pair of charged decay products with opposite electric charges can be attributed either to the decay channels with two charged leptons or to more frequent channels with two charged pions ($\eta \to \pi^+\pi^-\gamma$ and $\eta \to \pi^+\pi^-\pi^0$).

The following variables are used in the further data analysis:

- The invariant mass of a pair of oppositely charged particles (M_{ee}). The electron mass is used in the calculations. A clear peak at the lowest value is expected for e^+e^- pairs from Dalitz decays and from conversion of real photons in the detector material.

- The total invariant mass of all reconstructed decay products (for example $M(e^+e^-\gamma)$ or $M(3\pi^0)$). It was required to be consistent with the η mass.

- The missing mass of all decay products (MM_η). It should, within errors, be equal to the mass of the ^{3}He nucleus (2.808 GeV/c^2).

- The ratio between the momentum measured in the MDC and the energy of the shower in the electromagnetic calorimeter associated with the charged track ($R_{p/E}$). It permits to distinguish between $e^\pm$ and $\pi^\pm$ when the particles reach the electromagnetic calorimeter.

- The opening angle between two reconstructed real or virtual photons ($\theta_{\gamma\gamma*}$ or $\theta_{\gamma*\gamma*}$) and the relative azimuthal angle between the photons ($\Delta\phi_{\gamma\gamma*}$ or $\Delta\phi_{\gamma*\gamma*}$). The angles are given in the laboratory frame.

The separation of electrons from pions relies in the end on the kinematics of the reactions studied. Due to the large mass difference, the energy momentum conservation is violated with the wrong mass assignment. For example was the contribution of the background from $pd \rightarrow {}^3\mathrm{He}\pi^+\pi^-$ to the final selection of the $\eta \rightarrow e^+e^-$ reaction found to be negligible. Conversely do neither the kinematics or other particle identification methods allow us to distinguish pions from muons in the studied channels.

A. Normalization: $\eta \rightarrow \pi^0\pi^0\pi^0_D$ decay

In order to normalize the branching ratios of the η meson decays involving an e^+e^- pair, a monitoring process is needed to check the reconstruction efficiency for electrons and positrons. This is specially important since the experiment was split into short time slices distributed over a longer time. This data sample was analyzed already for a previous paper [6] on the $\eta \rightarrow \pi^+\pi^-e^+e^-$ decay mode where the $\eta \rightarrow \pi^+\pi^-\pi^0$ decay was used for the primary normalization. A cross check was done using $e^+e^-\gamma$ decays assuming the Particle Data Group (PDG) [7] value for this BR. To reduce the systematical uncertainty and in order to be able to determine the BR($e^+e^-\gamma$) we used in this paper both $\eta \rightarrow \pi^+\pi^-\pi^0$ and $\eta \rightarrow \pi^0\pi^0\pi^0_D$ decays for the normalization.

Dalitz decays of at least one of the three π^0's from the $\eta \rightarrow \pi^0\pi^0\pi^0$ decays provide an abundant data set of events with five photons and an electron-positron pair – $\eta \rightarrow \pi^0\pi^0\pi^0_D$. The Dalitz decay of the π^0 meson has been studied in detail both theoretically and experimentally. To select a data sample of $\eta \rightarrow \pi^0\pi^0\pi^0_D$ events we required:

- at least two tracks from particles with opposite charges
- more than three neutral hit clusters in the calorimeter.

In fig. 3 the experimental M_{ee} distribution for such events is plotted. The peak at low masses is attributed to the e^+e^- pairs from $\eta \rightarrow \pi^0\pi^0\pi^0$ decays with internal or external conversion of one of the photons (solid line in the fig. 3). The maximum at larger masses is due to η decays with a $\pi^+\pi^-$ pair, mainly the $\eta \rightarrow \pi^+\pi^-\pi^0$ decay. The relative normalization of the decays differs by 15% from what is expected from the branching ratios. This difference is attributed to the lower reconstruction efficiency for electrons and positrons than for charged pions in the MDC.

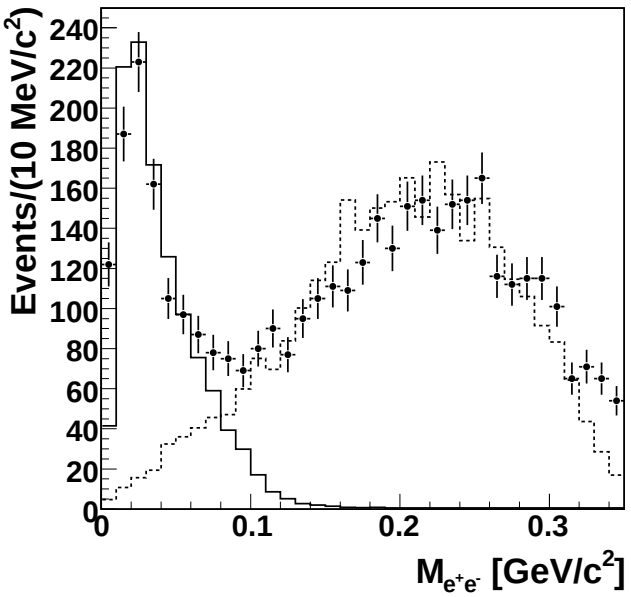

FIG. 3: Invariant mass of the e^+e^- candidates for events with more than three neutral hit clusters. Points – the experimental data, solid line – MC simulation for $\eta \rightarrow \pi^0\pi^0\pi^0_D$ decay, dotted line – background from decays involving a misidentified $\pi^+\pi^-$ pair.

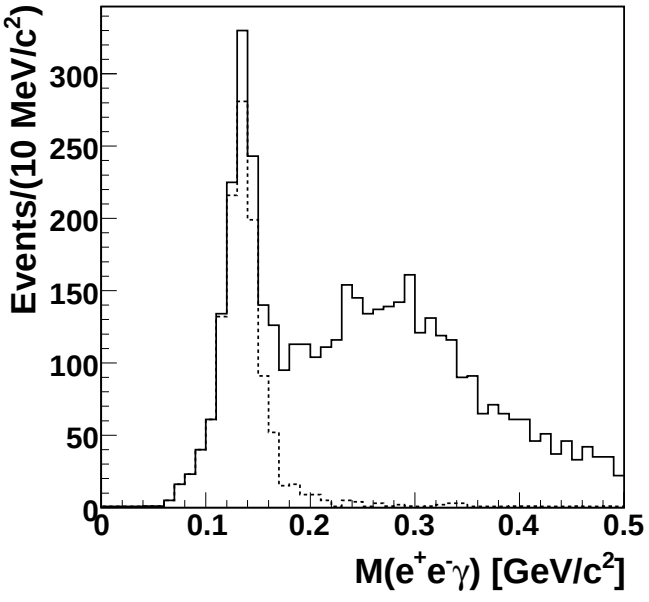

FIG. 4: The $e^+e^-\gamma$ invariant mass for events with at least four neutral hit clusters. Full line – all events, dotted line – events with e^+e^- invariant mass less than 0.1 GeV. The photon giving the $M(e^+e^-\gamma)$ mass closest to the neutral pion mass was selected.

The identification of the $\eta \to \pi^0\pi^0\pi^0_D$ decay channel is confirmed by the reconstruction of the invariant mass of the $e^+e^-\gamma$ system ($M(e^+e^-\gamma)$) where the photon leading to the mass value closest to the π^0 mass is selected (fig. 4). The $M(e^+e^-\gamma)$ distribution is peaked at the π^0 mass when the $M_{ee} < 0.1$ GeV/c^2 condition is applied. Fig. 5 shows the invariant mass of the three π^0's for the events where all pion energies are below 0.2 GeV. For the final data sample it was required that the missing mass of the system of all decay products is in the range 2.5 GeV/c^2 to 3.0 GeV/c^2 and the reconstructed emission angle of the η meson is less than 60°. Assuming that all remaining events are due to the decays of η into three neutral pions, the total number of η mesons N_η is calculated from the formula:

$$N_\eta = \frac{N_D}{(1-(1-p)^3)\mathcal{A}\ BR(\eta \to \pi^0\pi^0\pi^0)} \qquad (1)$$

where N_D is the number of the observed events (fig. 5 after background subtraction) and $p \equiv BR(\pi^0 \to e^+e^-\gamma) = (1.198 \pm 0.032)\%$ [7]. The product of the detector acceptance and the reconstruction efficiency ($\mathcal{A} = (13.8 \pm 2.0)\%$) was extracted from a MC simulation assuming the Vector Meson Dominance model Form Factor for the π^0. The value of $BR(\eta \to \pi^0\pi^0\pi^0)$ is precisely known – $(32.51 \pm 0.28)\%$ [7]. The extracted

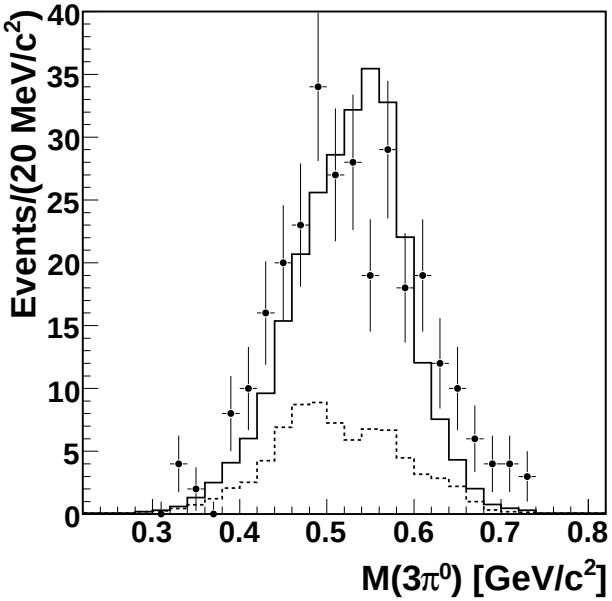

FIG. 5: The $M(3\pi^0)$ distribution for events with three neutral pions reconstructed after all cuts. Points – the experimental data, solid line – MC simulation for the sum of the $\eta \to \pi^0\pi^0\pi^0_D$ decay and the background, dashed line – $\eta \to \pi^0\pi^0\pi^0$ with external conversion.

$N_\eta = 256000 \pm 18000$ agrees with the value from our previous paper [6] within two standard deviations. Then, for the BR normalization in the present paper we use the weighted mean value: $N_\eta = 241000 \pm 13000$.

III. RESULTS

A. Single Dalitz decay $\eta \to e^+e^-\gamma$

Fig. 6 shows the invariant mass distribution of $e^+e^-\gamma$ candidates ($M(e^+e^-\gamma)$) selected by the following conditions:

- at least two tracks from particles with opposite charges
- for tracks with matched hit clusters in the calorimeter the condition $R_{p/E} < 1.65$ was applied
- $M_{ee} < 0.125$ GeV/c^2
- a neutral hit cluster with energy deposit larger than 180 MeV.

A clear signal at the $M(e^+e^-\gamma)$ around the η meson mass is seen. The solid line in Fig. 6 represent MC simulation of signal and a sum of all background contributions. External conversion of one of the photons from $\eta \to \gamma\gamma$ decay comprises the most important background as discussed in the section II. The MC underestimates the detector resolution in the $M(e^+e^-\gamma)$. The discrepancy is caused by not optimal calibration of the calorimeter which is difficult to improve since the data taking was distributed over a longer time. We have checked the influence of the effect on the extracted values of the BR by artificially smearing the MC distributions to match the experimental data.

There are no restrictions on the number of low energy neutral hit clusters since due to electron or photon interaction in the calorimeter an additional hit cluster can be created. For about 22% of the events, an additional low-energy neutral cluster is reconstructed. The photon candidate for the $\eta \to e^+e^-\gamma$ decay was selected by the requirement that the $\Delta\phi_{\gamma\gamma^*}$ angle is closest to 180°. The signature of the $\eta \to e^+e^-\gamma$ decay is an energetic photon ($E_\gamma > 0.18$ GeV). The opening angle $\theta_{\gamma\gamma^*}$ is distributed between 110° and 150° peaking around 130°. Fig. 7 shows $\theta_{\gamma\gamma^*}$ versus $M(e^+e^-\gamma)$. A constraint on the angle: $100° < \theta_{\gamma\gamma^*} < 160°$ together with a condition on the overall missing mass for the decay system 2.65 GeV/c^2 $< MM_\eta <$2.90 GeV/c^2 cleans the data sample significantly. This allows to release the condition on $R_{p/E} < 1.65$ and this increases the acceptance since not all e^+e- from $\eta \to e^+e^-\gamma$ decay reach the calorimeter. Finally 729 events with $M(e^+e^-\gamma)$ between 0.40 and 0.64 GeV/c^2 are identified. The total contribution of background (mainly from $\eta \to \pi^+\pi^-\gamma$, $\eta \to \pi^+\pi^-\pi^0$ and $\eta \to \gamma\gamma$ with one of the photons converting into e^+e^- pair in the detector material) is estimated to 294 ± 15 events. Fig. 8 shows the $M(e^+e^-\gamma)$ distribution after applying all selection cuts mentioned above.

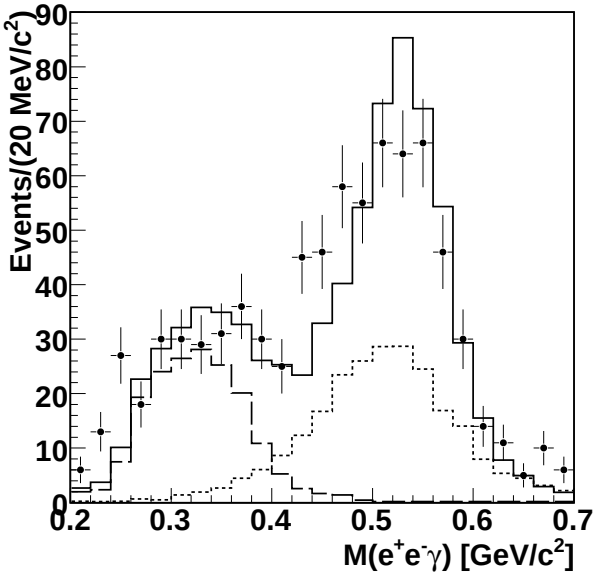

FIG. 6: The $M(e^+e^-\gamma)$ distribution for events with $M_{ee} < 0.125$ GeV/c^2 after particle identification. Points – data, solid line is the sum of MC simulations of the signal ($\eta \to e^+e^-\gamma$) and the background. Dashed line – contribution from $\eta \to \pi^+\pi^-\pi^0$ and $\eta \to \pi^+\pi^-\gamma$ decays; dotted line – $\eta \to \gamma\gamma$ with one of the photons converted into e^+e^- pair in the detector material.

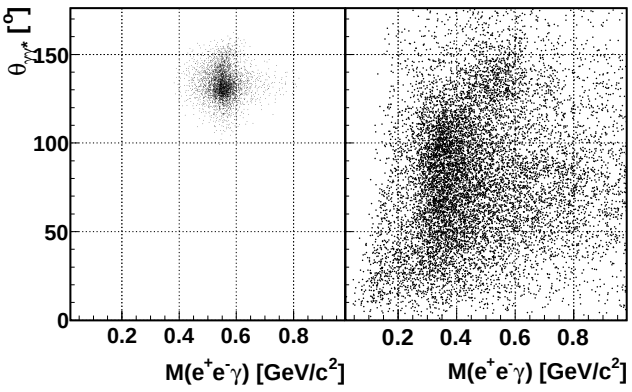

FIG. 7: $\theta_{\gamma\gamma*}$ vs $M(e^+e^-\gamma)$ before cleaning cuts and without particle identification: left – MC simulation for $\eta \to e^+e^-\gamma$, right – experimental data candidates.

B. The decay $\eta \to e^+e^-e^+e^-$

In a search for the $\eta \to e^+e^-e^+e^-$ decay, events with exactly two positively and two negatively charged particle tracks in the MDC were selected. According to the simulations 11% of the reconstructed $\eta \to e^+e^-e^+e^-$ events should fulfill the following criteria:

- the relative angle between electron and positron in both pairs is smaller than 40°

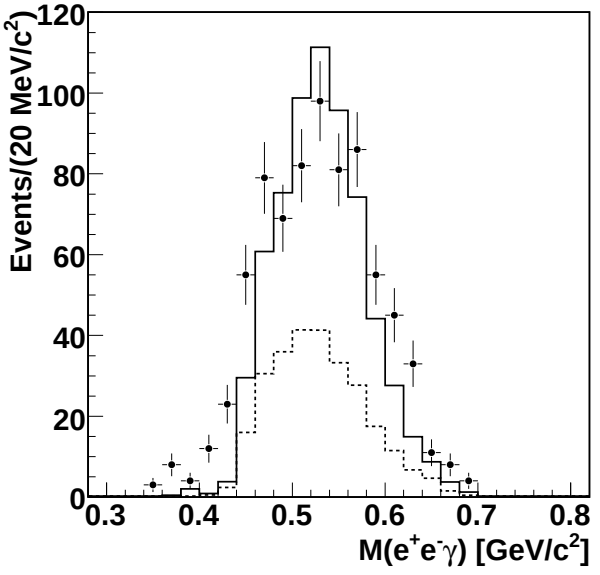

FIG. 8: The $M(e^+e^-\gamma)$ distribution after the final selection. Points – experimental data, solid line – MC simulation of $\eta \to e^+e^-\gamma$, dotted line – MC simulation of $\eta \to \gamma\gamma$ with photon conversion in the detector material.

- the opening angle between the momenta of the two e^+e^- pairs is in the interval 110° to 170°
- the η meson emission angle is smaller than 45°
- the missing transverse momentum is less than 0.3 GeV/c.

In the data only two events passed all selection cuts. The event display for one of the two candidates is shown in fig. 9.

The background is estimated to 1.3 ± 0.2 events and originates mainly from single Dalitz decay $\eta \to e^+e^-\gamma$ with the photon converting into an e^+e^- pair in the detector material.

C. The decays $\eta \to \mu^+\mu^-\mu^+\mu^-$ and $\eta \to \pi^+\pi^-\mu^+\mu^-$

The decays $\eta \to \mu^+\mu^-\mu^+\mu^-$ and $\eta \to \pi^+\pi^-\mu^+\mu^-$ have very similar kinematics. In the analysis we have focused on the $\eta \to \mu^+\mu^-\mu^+\mu^-$ decay but it is not possible to distinguish the two in the present analysis. One starts with a similar sample of events as for the $\eta \to e^+e^-e^+e^-$ decay analysis: four tracks from charged particles with charge balance. The events with neutral hit clusters of energy larger than 20 MeV or with a track in the Forward Detector (detection angle 2°–17°) are rejected. The kinematics is checked assuming muon mass for the four charged particles. The opening angle between the momenta of the two muon pairs is required to be in the interval 26°–163°. No candidate event for the discussed

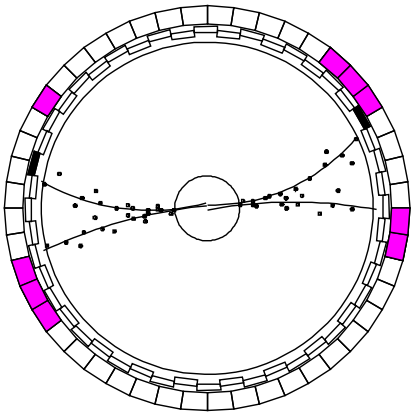

FIG. 9: (Color online) Event display for an $\eta \to e^+e^-e^+e^-$ candidate event. The shaded area in the outermost ring represents the projection of the hit calorimeter crystals (the size of the crystals and the radial position of the front faces are not to scale). The lines represent the reconstructed tracks from the pattern recognition program. In addition to layers with straws along the beam, the MDC includes twisted layers which cause the spread of points for forward/backward going tracks.

decay channels is left for four candidate muons with invariant mass less than 0.625 GeV/c^2 and a missing mass MM$_\eta$ greater than 2.32 GeV/c^2.

D. The decay $\eta \to e^+e^-$

Events with two tracks from charged particles of opposite charge are considered. The $\eta \to e^+e^-$ decay has a distinctive signature in the $pd \to {}^3\mathrm{He}\,\eta$ reaction close to threshold: the emitted electron and positron have large energies ($E > 150$ MeV), are co-planar with the beam and have a large opening angle (about 130°). In fig. 10, the e^+e^- invariant mass is presented as a function of the opening angle between the electron and positron for the whole data set. The region of the simulated signal after reconstruction cuts is also shown. There are no events in the region where the majority of the $\eta \to e^+e^-$ signal is expected: e^+e^- opening angle in the interval 120°–160°, $M_{ee} > 0.49$ GeV/c^2 and fulfilling the particle identification criteria $0.5 < R_{p/E} < 1.65$.

E. Discussion

The results of the experiment are summarized in table II. The values of the branching ratios are presented in table III. The confidence limits and intervals for decays 1–4 were extracted using Feldman and Cousins prescription for small signals with background [25].

The systematical errors were obtained by varying cuts applied for selection of the channels and comparison with Monte Carlo studies including e.g. different assumptions

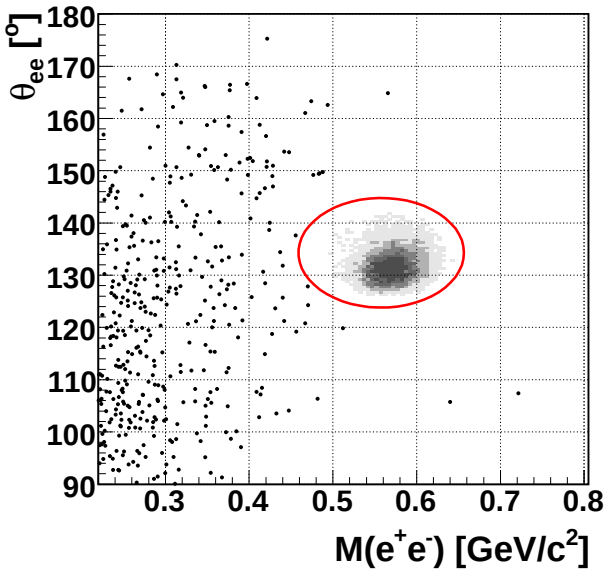

FIG. 10: (Color online) Opening angle between electron and positron tracks vs M_{ee} for $\eta \to e^+e^-$ event sample selection: scatter plot – data; shaded area – MC simulation of the $\eta \to e^+e^-$ decay. A cut corresponding to the ellipse shown in the figure, selects 71% of the simulated $\eta \to e^+e^-$ events accepted in the plot.

Decay mode	$\mathcal{A}$	Events background	Events observed
1. $\eta \to e^+e^-e^+e^-$	(11±1)%	1.3±0.2	2
2. $\eta \to \mu^+\mu^-\mu^+\mu^-$	(5±1)%	1.4±0.9	0
3. $\eta \to \pi^+\pi^-\mu^+\mu^-$	(5±1)%	1.4±0.9	0
4. $\eta \to e^+e^-$	(36±3)%	0.4±0.1	0
5. $\eta \to \pi^+\pi^-e^+e^-$	(16±1)%	7.7±2.0	24
6. $\eta \to e^+e^-\mu^+\mu^-$	(16±2)%	21.0±2.5	24
7. $\eta \to e^+e^-\gamma$	(23±2)%	294±15	729

TABLE II: The detector acceptance $\mathcal{A}$ (reconstruction efficiency included), expected number of background events and the number of the observed events after all selection cuts.

Decay mode	BR	BR limit 90% CL
1. $\eta \to e^+e^-e^+e^-$	$(2.7^{+2.1}_{-2.7}{}_{stat} \pm 0.1_{syst})\times10^{-5}$	$<9.7\times10^{-5}$
2. $\eta \to \pi^+\pi^-\mu^+\mu^-$	–	$<3.6\times10^{-4}$
3. $\eta \to \mu^+\mu^-\mu^+\mu^-$	–	$<3.6\times10^{-4}$
4. $\eta \to e^+e^-$	–	$<2.7\times10^{-5}$
5. $\eta \to \pi^+\pi^-e^+e^-$	$(4.3^{+2.0}_{-1.6}{}_{stat} \pm 0.4_{syst})\times10^{-4}$	–
6. $\eta \to e^+e^-\mu^+\mu^-$	–	$<1.6\times10^{-4}$
7. $\eta \to e^+e^-\gamma$	$(7.8\pm0.5_{stat}\pm0.8_{syst})\times10^{-3}$	–

TABLE III: Final results for the branching ratios of lepton η decays.

on photon energy reconstruction in the calorimeter and on the contribution of interaction with rest gas. The main sources of the systematical uncertainty are:

1. Uncertainty on the total number of the η mesons in our data sample. That value is dominated by a limited number of collected $\eta \to \pi^0\pi^0\pi^0_D$ and $\eta \to \pi^+\pi^-\pi^0$ decays. Moreover the systematical errors of the acceptance and reconstruction efficiency and BR for these channels were taken into account. This contributes with 5.4% to the relative uncertainty of the BR for all channels.

2. Uncertainty of the background contribution.

3. Acceptance and reconstruction efficiency uncertainty for a given channel. By using simultaneously collected data with similar topologies for normalization, the contribution of uncertainty of track reconstruction efficiency is partly canceled.

For example in the case of $\eta \to e^+e^-\gamma$ decay the systematical error is dominated by the uncertainty in the acceptance ($\Delta\mathcal{A}/\mathcal{A} = 8\%$) and it is estimated from the discrepancy between the data and the MC.

The extracted signal for the $\eta \to e^+e^-\gamma$ decay, $435 \pm 27_{stat} \pm 15_{syst}$ events, leads to BR($\eta \to e^+e^-\gamma$)=$(7.8 \pm 0.5_{stat} \pm 0.8_{syst}) \times 10^{-3}$. This is 20% larger than theoretical estimates. The result is in between the PDG value and the latest CLEO result [13].

The attempt to extract a branching ratio from the observed two $\eta \to e^+e^-e^+e^-$ event candidates leads to the value $(2.7^{+2.1}_{-2.7 stat} \pm 0.1_{syst}) \times 10^{-5}$ which is in good agreement with theoretical estimates. However due to non negligible background the value is also consistent with zero. If instead one assumes that the events are due to background, the upper limit is 9.7×10^{-5} (90% CL). This improves slightly the previous limit from CMD-2 [3]. The background is mainly due to conversion of the photon from the $\eta \to e^+e^-\gamma$ decay in the beam tube. It could be reduced by checking the position of the reconstructed vertex or by selecting events with larger invariant masses of the e^+e^- pairs. This however decreases the acceptance significantly and could not be done in the present study.

The extracted upper limit for BR($\eta \to e^+e^-$) is 2.7×10^{-5} (90% CL) and is two times lower than the previous one from the CLEO II experiment.

We also report on the first search for the decays $\eta \to \mu^+\mu^-\mu^+\mu^-$ and $\eta \to \pi^+\pi^-\mu^+\mu^-$. Since the decays can not be distinguished in the present data analysis an upper limit of 3.6×10^{-4} (90% CL) can be given for the sum of the decay branching ratios. Similarly $\eta \to \pi^+\pi^-e^+e^-$ and $\eta \to e^+e^-\mu^+\mu^-$ decays were not distinguished in the previous analysis of $\eta \to \pi^+\pi^-e^+e^-$ decay [6]. However the branching ratio of the $\eta \to e^+e^-\mu^+\mu^-$ decay is expected to be three orders of magnitude lower. Assuming that BR($\eta \to \pi^+\pi^-e^+e^-$) is given as the average of theoretical predictions, $(3.3\pm0.3)\times10^{-4}$ [8, 9, 10, 12], and taking into account the other sources of background reported in [6] a limit for the BR($\eta \to e^+e^-\mu^+\mu^-$) to 1.6×10^{-4} (90% CL) is obtained. For consistency reasons we have also reevaluated the result on BR($\eta \to \pi^+\pi^-e^+e^-$) using the Feldman and Cousins approach and the improved normalization (table III).

Acknowledgments

We are grateful to the personnel at The Svedberg Laboratory for their support during the course of the experiment. The financial support from the Knut and Alice Wallenberg Foundation (Sweden), the Swedish Research Council and the Göran Gustafsson Foundation (Sweden) is acknowledged. This work has also been supported by BMBF (Germany) (grants 06HH152, 06TU261), by Russian Foundation for Basic Research (grant RFBR 02-02-16957) and by the European Community Research Infrastructure Activity under FP6, Hadron Physics, RII-CT-2004-506078 and HPRI-CT-1999-00098.

[1] R. H. Dalitz, Proc. Phys. Soc. **A64**, 667 (1951).
[2] L. G. Landsberg, Phys. Rept. **128**, 301 (1985).
[3] R. R. Akhmetshin et al. (CMD-2), Phys. Lett. **B501**, 191 (2001), hep-ex/0012039.
[4] T. E. Browder et al. (CLEO), Phys. Rev. **D56**, 5359 (1997), hep-ex/9706005.
[5] L. Bergström, Zeit. Phys. **C14**, 129 (1982).
[6] C. Bargholtz et al. (CELSIUS/WASA), Phys. Lett. **B644**, 299 (2007), hep-ex/0609007.
[7] W. M. Yao et al. (Particle Data Group), J. Phys. **G33**, 1 (2006).
[8] C. Jarlskog and H. Pilkuhn, Nucl. Phys. **B1**, 264 (1967).
[9] C. Picciotto and S. Richardson, Phys. Rev. **D48**, 3395 (1993).
[10] A. Faessler, C. Fuchs, and M. I. Krivoruchenko, Phys. Rev. **C61**, 035206 (2000), nucl-th/9904024.
[11] J. Bijnens and F. Borg (1999), hep-ph/0106130.
[12] B. Borasoy and R. Nissler, Eur. Phys. J. **A33**, 95 (2007), arXiv:0705.0954 [hep-ph].
[13] A. Lopez et al. (CLEO) (2007), arXiv:0707.1601 [hep-ex].
[14] S. D. Drell, Nuovo Cimento **11**, 693 (1959).
[15] D. Gomez Dumm and A. Pich, Phys. Rev. Lett. **80**, 4633 (1998), hep-ph/9801298.
[16] G. Isidori and R. Unterdorfer, JHEP **01**, 009 (2004), hep-ph/0311084.
[17] M. J. Savage, M. E. Luke, and M. B. Wise, Phys. Lett. **B291**, 481 (1992), hep-ph/9207233.
[18] L. Ametller, A. Bramon, and E. Masso, Phys. Rev. **D48**, 3388 (1993), hep-ph/9302304.
[19] E. Abouzaid et al. (KTeV), Phys. Rev. **D75**, 012004 (2007), hep-ex/0610072.
[20] A. E. Dorokhov and M. A. Ivanov, Phys. Rev. **D75**,

114007 (2007), arXiv:0704.3498 [hep-ph].
[21] Y. Kahn, M. Schmitt, and T. Tait (2007), arXiv:0712.0007 [hep-ph].
[22] J. Zabierowski et al. (CELSIUS/WASA), Phys. Scripta **T99**, 159 (2002).
[23] C. Ekström (CELSIUS/WASA), Phys. Scripta **T99**, 169 (2002).
[24] C. Bargholtz et al., Nucl. Instrum. Meth. **A390**, 160 (1997).
[25] G. J. Feldman and R. D. Cousins, Phys. Rev. **D57**, 3873 (1998), physics/9711021.